J. of Supercritical Fluids 110 (2016) 56–64

Contents lists available at ScienceDirect

The Journal of Supercritical Fluids

journal homepage: www.elsevier.com/locate/supflu

High pressure solubility of CH_4, N_2O and N_2 in 1-butyl-3-methylimidazolium dicyanamide: Solubilities, selectivities and soft-SAFT modeling

Luís M.C. Pereira[a], Vânia Martins[a], Kiki Adi Kurnia[b], Mariana B. Oliveira[a], Ana M.A. Dias[c], Felix Llovell[e,f], Lourdes F. Vega[d,e], Pedro J. Carvalho[a], João A.P. Coutinho[a,*]

[a] CICECO – Aveiro Institute of Materials, Department of Chemistry, University of Aveiro, 3810-193 Aveiro, Portugal
[b] Center of Research in Ionic Liquids, Department of Chemical Engineering, Universiti Teknologi PETRONAS, Tronoh 31750, Perak, Malaysia
[c] CIEPQPF, Departamento de Engenharia Química, FCTUC, University of Coimbra, Rua Sílvio Lima, Pôlo II—Pinhal de Marrocos, 3030-790 Coimbra, Portugal
[d] Alya Technology & Innovation, Centre de Promoció Empresarial, C/Tres Creus, 236, 08203 Sabadell, Barcelona, Spain
[e] MATGAS Research Center, Campus UAB, Bellaterra, 08193, Barcelona, Spain
[f] IQS School of Engineering, Universitat Ramon Llull, Via Augusta, 390, 08017 Barcelona, Spain

ARTICLE INFO

Article history:
Received 27 October 2015
Received in revised form
10 December 2015
Accepted 11 December 2015
Available online 15 December 2015

Keywords:
Methane
Nitrous oxide
Nitrogen
1-Butyl-3-methylimidazolium dicyanamide
High pressure
Henry's constant
Solubility
Selectivity
Soft-SAFT EoS

ABSTRACT

The society and industry commitment to progressively reduce Green House Gases (GHGs) emissions forged important challenges that conventional gas separation processes are unable to overcome. Ionic liquids (ILs) have been attracting an outstanding attention during the last decade as a promising class of viable solvents to capture pollutants and for gas separation processes. Being the IL-based membranes gas separation controlled by the gas solubility in the IL rather than by its diffusivity, the solubility of gases in ILs stands as highly relevant input for their application in liquid membranes. As part of a continuing effort to develop an IL based process for high pressure capture of GHGs, the phase equilibria of nitrous oxide (N_2O), methane (CH_4) and nitrogen (N_2) were investigated in this work. Experimental gas–liquid equilibrium data for N_2O, CH_4 and N_2 in $[C_4C_1im][N(CN)_2]$ were determined in the (293 to 363) K temperature range, for pressures up to 70 MPa and gas mole fractions up to 35 %.

Unfavorable interactions towards the studied gases, with positive deviations to ideality, were observed for all the studied gases, placing the studied IL among those with the lowest selectivities reported. The observed behavior highlights that a delicate balance between the solvent polarity and its molar volume must be ascertained when a highly selective solvent for N_2 or CH_4 separation is envisaged. The soft-SAFT EoS successfully described the high pressure phase behavior data using the molecular model and parameters sets reported in previous works. A good description of the binary systems studied, including the small CH_4 temperature dependency and the N_2 reverse temperature dependency on the solubility were achieved using just one binary interaction parameter. This reinforces the use of soft-SAFT as an accurate model to describe the behavior of gases in ILs for different applications.

1. Introduction

Several anthropogenic or natural origin sources, contribute to air pollution but, among them burning of fossil fuels and industrial processes stand as those with the highest impact. Among the several post-combustion capture and natural gases treatment processes available, like membrane-based separations and sorbents for physical and chemical adsorption, the amines and ammonia absorption maintain a prominent position, since the majority of the industrial plants use monoethanolamine (MEA)-based solvents for gas chemical absorption [1,2]. Although these MEA-based processes have been modified to incorporate inhibitors, to reduce solvent degradation and equipment corrosion, they still present several disadvantages, like large equipment sizes (due to low amines/water weight ratio) and high solvent regeneration costs, just to mention a few. Furthermore, limitations on the existing control methods and on the industrial processes demand for the development of new methods and processes to reduce the emission of such pollutants.

* Corresponding author. Tel.: +351 234 401 507; fax: +351 234 370 084.
E-mail address: jcoutinho@ua.pt (J.A.P. Coutinho).

http://dx.doi.org/10.1016/j.supflu.2015.12.006
0896-8446/

Ionic liquids (ILs), due to their outstanding properties and aptness for fine-tuning their properties, appear today as viable alternatives to replace commonly used solvents in natural gas and post-combustion treatments. Moreover, ILs-based liquid membranes, with high fluxes and high selectivities, are being reported as a promising method for gas separations [3–5]. Furthermore, gas separation using IL-based membranes seems to be controlled by the gas solubility in the ionic liquid rather than by its diffusivity and therefore, the solubility of gases in ILs have received a great deal of attention in the past decade [6–9]. The idea that the IL-gas solubility is related to the IL polarity has been proposed and supported in previous works [10–12] where the mechanism behind the sorption of several gases in ILs has been discussed. However, the endless possible combinations of IL's cations and anions limit the feasibility of the experimental characterization of all the ILs. Thus, the development of reliable thermodynamic models capable of estimating the solubility of gases in ILs stands as an essential key in the pursuit for alternative solvents for gas/pollutants sorption processes.

One of the most successful thermodynamic models developed and applied for the description of pure ILs and their mixtures with gases is the soft-SAFT (Statistical Associating Fluid Theory) EoS [13,14]. The great success of this SAFT-type equation, relies on its ability to provide consistent predictions for the phase equilibria and thermophysical properties of ILs and ILs-based systems using transferable molecular parameters for the pure compounds and just one or two binary interaction parameters, in the case of IL-based mixtures, independently of the system compounds and pressure and temperature conditions [15]. In a previous work, Pereira et al. [16] modeled the N_2O and CO_2 solubilities in various $[C_4C_1im]^+$ based ILs using the soft-SAFT. Proper coarse-grained molecular models and parameters sets were proposed for each ionic liquid based on structural information, guided by quantum calculations and previous experience. The proposed molecular parameters were able to correctly describe experimetal high pressure gas-IL equilibrium (GLE) data without using any binary interaction parameter and, whenever needed, using temperature independent binary parameters. One of the ILs studied in that work was the 1-butyl-3-methylimidazolium dicyanamide. This compound is interesting given its basicity and strong hydrogen bonding character and has been intensively studied in our lab both for its thermophysical properties [17,18] and its interactions with water and alcohols. The later have been experimentally and theoretically, using molecular dynamics simulations, investigated [19] revealing the particular behavior of 1-butyl-3-methylimidazolium dicyanamide among the cyano containing ionic liquids.

Aiming at continuing to explore the behavior of 1-butyl-3-methylimidazolium dicyanamide and the development of a molecular-based Equation of State with predictive capability, applicable to the description of the phase behavior and thermophysical properties of different types of compounds, the soft-SAFT EoS is here extended to the description of the high pressure gas–liquid equilibria of methane (CH_4), nitrogen (N_2) and nitrous oxide (N_2O) in 1-butyl-3-methylimidazolium dicyanamide measured in this work.

2. Modeling

The soft-SAFT EoS equations have been shown in detail in previous publications [13]. With its chain and associating terms based on the Wertheim's first-order perturbation theory, as happens with others variants of SAFT, soft-SAFT reference term consists on a Lennard-Jones spherical fluid that takes into account the repulsive and attractive interactions of the monomers constituting the chain. The structural information of the reference fluid is introduced into the chain and the associating term following a thermodynamic perturbative approach.

2.1. Molecular model

The key element for the accurate prediction of the phase equilibria and thermophysical properties from molecular-based EoSs is the selection of a reliable coarse-grained model that can represent the basic physical features of the compound(s) to be described. Soft-SAFT EoS relies on the pre-selection of a molecular model for the pure compounds. Non-associating molecules are defined by three molecular parameters: the chain length, m_i, the segment diameter, σ_{ii}, and the dispersive energy between segments, ε_{ii}/k_B. Linear symmetrical molecules involve two additional molecular parameters: the quadrupolar moment, Q, and the fraction of segments in the chain that contains the quadrupole, x_P. Finally, for associating molecules two more parameters are included to model the associating interactions: the site-site association energy, $\varepsilon^{HB}_{\alpha\beta,ij}/k_B$, and the site–site bonding – volume of association, $K_{\alpha\beta,ij}$.

The CO_2, CH_4, N_2O and N_2 molecular parameters were taken from previous works [20–23] and are presented in Table 1 As can be seen, CO_2, N_2O and N_2 were modeled as LJ chains in which explicit quadrupolar interactions were taken into account with the molecular parameter x_P fixed to 1/3 for CO_2 and N_2O and to 1/2 for N_2, representing the number of segments in those molecules (three and two, respectively) that may momentarily contain the quadrupole [20,21,24].

In a previous work [16] a detailed study of the appropriate $[C_4C_1im][N(CN)_2]$ molecular model and parameters set was performed. From quantum calculations, IL density and CO_2 and N_2O solubility results let to a coarse-grained model for this ionic liquid as an associating molecule with two associating sites, one (**A**) representing the N-atom interactions with the cation and the other (**B**) representing the delocalized charge due to the two extra N-atoms on the anion. The best set of molecular parameters assigned for this ionic liquid is presented in Table 1.

3. Experimental

3.1. Materials

The ionic liquid 1-butyl-3-methylimidazolium dicyanamide, $[C_4C_1im][N(CN)_2]$, was obtained from Io-li-tec with mass fraction purities higher than 98 %. The IL was further purified through a drying process under high vacuum (0.1 Pa) and moderate temperature (323 K) for a minimum period of 48 h in order to reduce both water and volatile compounds to negligible values. The purities of the ionic liquid were verified by ^1H NMR and ^{13}C NMR after the purification step and estimated to be higher than 99 %. The final IL water content was determined with a Metrohm 831 Karl Fischer coulometer, indicating a water mass fraction of 37×10^{-6}.

Methane (CH_4) was acquired from Air Liquide with a purity of ≥99.998 % and the nitrous oxide (N_2O) and Nitrogen (N_2) from Praxair with a purity of ≥99.998 %.

3.2. Experimental equipment

Both the apparatus and the methodology used in this work were fully described previously [25] and shown to adequately and accurately measure gas–liquid equilibrium for a wide range of fluids, pressures and temperatures. The high pressure equilibrium cell is based on a cell designed by Daridon et al. [26,27] and consists of a horizontal hollow stainless-steel cylinder, closed at one end with a movable piston and at the other end with a sapphire window, from which the operator follows the behavior of the sample with

Table 1
Soft-SAFT EoS molecular parameters for the studied compounds.

	m	σ (Å)	ε/k_B (K)	ε^{HB}/k_B (K)	k^{HB} (Å^3)	Q (C m^2)	Ref.
CO_2	1.571	3.184	160.20	–	–	4.1 × 10−40	[20]
N_2	1.205	3.384	89.16	–	–	1.2 × 10−40	[21]
CH_4	1.000	3.728	147.20	–	–	–	[22]
N_2O	1.656	3.153	159.83	–	–	4.1 × 10−40	[23]
$[C_4C_1im][N(CN)_2]$	5.700	3.754	384.28	3850	2450		[16]

pressure and temperature. The temperature is measured with a Pt100 thermometer with an uncertainty of 0.15 K and placed inside the cell close to the sample. The cell is thermostatized by circulating a heat-carrier fluid thermo-regulated, with a temperature stability of ±0.01 K, by means of a thermostat bath circulator (Julabo MC), through three flow lines directly managed into the cell. The pressure is measured by a piezoresistive silicon pressure transducer (Kulite HEM 375) fixed directly inside the cell, to reduce dead volumes, that was previously calibrated and certified by an independent laboratory with IPAC accreditation, following the EN 837-1 standard and with an accuracy better than 0.2 %. The homogenization of the mixture is held by a small magnetic bar placed inside the cell and an external magnetic stirrer.

According to the applied synthetic method, a fixed amount of IL, whose exact mass is determined by weight using a high weight/high precision balance (Sartorius LA200P) with an accuracy of 1 mg, is introduced inside the cell. The IL is then kept under vacuum overnight, while stirring and heating at 353 K, in order to remove atmospheric gases absorbed during manipulation. The gas is introduced under pressure, from an ultra-lightweight composite cylinder, by means of a flexible pressure capillary and its mass measured with a high weight/high precision balance.

After preparation of a mixture with known composition, the pressure is then slowly increased at a given and previously defined and stabilized temperature, until the system becomes monophasic. The pressure at which the last bubble disappears represents the equilibrium pressure at the fixed temperature and composition.

The purity of the IL is checked again by NMR at the end of the study to confirm that no degradation occurred during the measurements.

4. Results and discussion

4.1. Nitrous oxide solubility

The solubility of nitrous oxide was measured for mole fractions ranging from (0.026 to 0.303), in the temperature range 293 to 363 K and pressures from 0.2 to 11 MPa, as reported in Table 2 and depicted in Fig. 1. The solubility of N_2O is similar to that of CO_2, reported in a previous publication [28], also presenting an increase on the equilibrium pressures as the temperature and gas concentration increase.

In the previous work [16], where the appropriate soft-SAFT molecular model and parameters were assigned for $[C_4C_1im][N(CN)_2]$, the equation of state was able to provide a very good prediction of the CO_2 solubility in $[C_4C_1im][N(CN)_2]$ for temperatures between 283 and 348 K and with no binary adjustable parameters required. The predictive ability of the soft-SAFT EoS is here tested by extending it to N_2O solubility data in the 293 to 363 K temperature range and mole fraction compositions up to 0.3, as represented in Fig. 1. Even though the EoS over-predicts the nitrous oxide solubility for gas mole fractions and temperatures higher than 0.2 and 333 K, it provides good predictions for the low gas concentration region and allows to accurately determine the Henry's constants. Furthermore and as previously reported, the EoS predicts a liquid–liquid region with a low critical solution temperature (LCST) at a temperature of about 257 K. The end of the VLLE region, i.e. the temperature of the critical endpoint (CEP), is predicted at approximately 326 K.

Experimental *pTx* data for the system $N_2O + [C_4C_1im][N(CN)_2]$ was previously reported by Shiflett et al. [29] using a gravimetric micro-balance from 283 to 348 K and for pressures up to 2 MPa. As depicted in Fig. 2 the data measured in this work are in good agreement over the entire composition range, with pressure deviations that varies from 0.04 to 1.05 MPa.

4.2. Methane solubility

The solubility of methane was measured for mole fractions ranging from 0.01 to 0.06, in the temperature range 293 to 363 K and pressures from 2 to 20 MPa, as reported in Table 3 and depicted on Fig. 3. The results show that, in accordance with previously reported data for other CH_4–IL systems [10,23], the temperature increase, although leading to the equilibrium pressure increase, has a small impact on the CH_4 solubility.

Despite the small temperature dependency experimentally observed for the solubility of CH_4 in $[C_4C_1im][[N(CN)_2]$, it was necessary to use a temperature dependent size binary interaction parameter to properly describe the experimental results with the soft-SAFT EoS (Fig. 3) in order to incorporate the size differences between the two components. This was done through the inclusion of a second order temperature dependent η parameter, described by:

$$\eta = 2.013 \cdot 10^{-6} T^2 - 1.120 \cdot 10^{-3} T + 1.207 \quad (1)$$

The energy parameter has little influence in the soft-SAFT results, meaning that the model is able to correctly take into account the weak interactions between CH_4 and $[C_4C_1im][[N(CN)_2]$ and therefore was not used. Similar behavior was previously observed for the $CH_4 + [C_2C_1im][CH_3OHPO_2]$ system [23].

4.3. Nitrogen solubility

The solubility of nitrogen was measured for mole fractions ranging from (0.018 to 0.085), in the temperature range 293 to 363 K and pressures from 7 to 69 MPa, as reported in Table 4 and depicted in Fig. 4. Contrary to what was observed for the other studied gases, the temperature increase leads to a decrease on the equilibrium pressures but at a much less pronounced rate, suggesting that this system presents a very low enthalpy of solution, as observed by Kumełan et al. [30] for some H_2 + ILs systems and more recently by our group for some CH_4 + ILs systems [10,23].

The results obtained with the soft-SAFT EoS to describe the solubility of N_2 in $[C_4C_1im][[N(CN)_2]$ were equivalent to those reported for N_2 in $[C_2C_1im][CH_3OHPO_2]$ [23]. The size binary parameter had little influence in the model results for the phase equilibria but a temperature independent energy binary interaction parameter equal to 0.88 was required to achieve the results depicted in Fig. 4.

Table 2
Bubble point data of the system N_2O + $[C_4C_1im][N(CN)_2]$.

x_{N_2O}	T (K)	p (MPa)	x_{N_2O}	T (K)	p (MPa)	x_{N_2O}	T (K)	p (MPa)
$m = 0.128\ mol_{N_2O} \cdot kg_{IL}^{-1}$			$m = 0.586\ mol_{N_2O} \cdot kg_{IL}^{-1}$			$m = 1.237\ mol_{N_2O} \cdot kg_{IL}^{-1}$		
0.026	293.44	0.20	0.107	293.42	1.04	0.202	293.68	2.11
	303.18	0.26		303.30	1.14		303.31	2.41
	313.39	0.31		313.11	1.31		313.46	3.01
	323.16	0.35		323.21	1.53		323.51	3.41
	332.94	0.39		333.32	1.68		333.28	3.96
	343.20	0.44		343.34	1.98		343.22	4.63
	353.02	0.51		353.41	2.26		353.10	5.24
	362.84	0.64		363.52	2.58		363.34	5.91
$m = 2.115\ mol_{N_2O} \cdot kg_{IL}^{-1}$								
0.303	-	-						
	303.46	4.31						
	312.92	5.21						
	323.05	6.08						
	333.14	7.27						
	343.13	8.25						
	353.50	9.47						
	363.41	10.65						

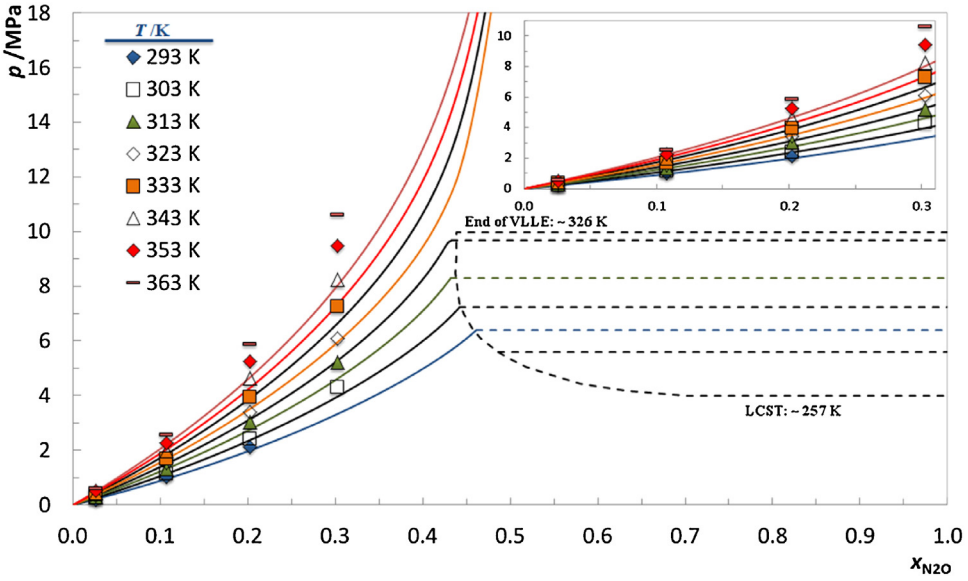

Fig. 1. *pTx* diagrams and modeling results for the system N_2O + $[C_4C_1im][N(CN)_2]$. The solid lines represent the soft-SAFT EoS predictions.

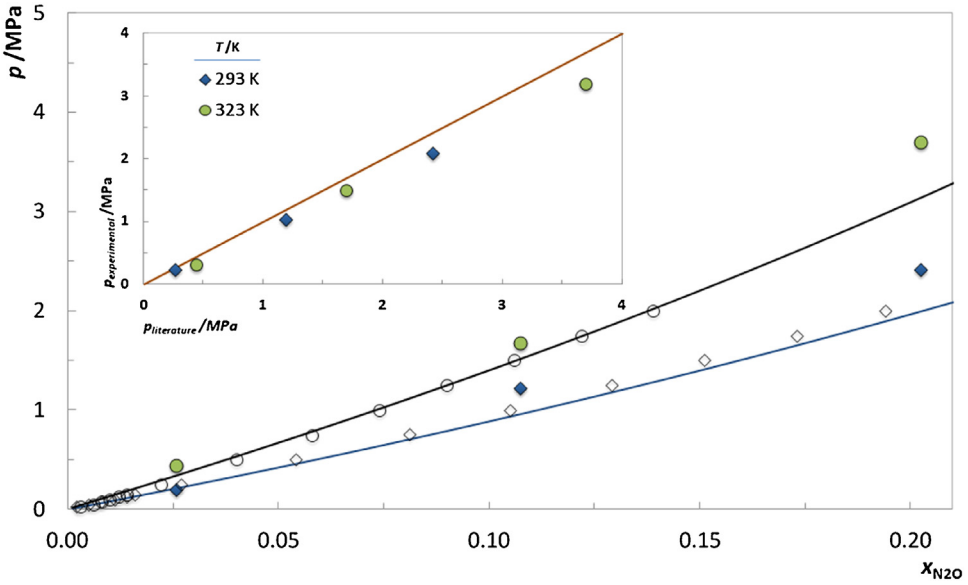

Fig. 2. *pTx* diagrams and modeling results for the system N_2O + $[C_4C_1im][N(CN)_2]$. The solid lines represent the soft-SAFT EoS predictions, and the symbols represent the data measured in this work (filled symbols) and that reported by Shiflett et al. [29] (empty symbols) at 298 K, respectively.

Table 3
Bubble point data for the system CH_4 + [C_4C_1im][N(CN)$_2$].

x_{CH_4}	T (K)	p (MPa)	x_{CH_4}	T (K)	p (MPa)	x_{CH_4}	T (K)	p (MPa)
$m = 0.041\ mol_{CH_4} \cdot kg_{IL}^{-1}$			$m = 0.095\ mol_{CH_4} \cdot kg_{IL}^{-1}$			$m = 0.150\ mol_{CH_4} \cdot kg_{IL}^{-1}$		
0.008	293.34	0.426	0.019	293.18	1.61	0.030	293.17	4.24
	303.07	0.427		303.19	1.83		303.19	4.42
	313.11	0.428		313.28	2.05		313.17	4.59
	323.17	0.429		323.24	2.13		323.17	4.68
	332.85	0.430		333.17	2.38		333.19	4.82
	343.13	0.431		343.19	2.41		343.21	4.97
	351.70	0.431		353.24	2.57		353.18	5.14
	363.07	0.432		363.12	2.68		363.19	5.25
$m = 0.209\ mol_{CH_4} \cdot kg_{IL}^{-1}$			$m = 0.263\ mol_{CH_4} \cdot kg_{IL}^{-1}$			$m = 0.368\ mol_{CH_4} \cdot kg_{IL}^{-1}$		
0.041	293.21	7.16	0.051	293.15	9.26	0.070	293.20	13.80
	303.16	7.34		303.65	9.50		303.20	13.88
	313.16	7.51		313.15	9.70		313.25	14.05
	323.18	7.81		322.55	10.07		323.25	14.17
	333.12	7.84		333.05	10.14		333.45	14.11
	343.17	7.92		343.75	10.29		343.55	14.20
	353.17	8.11		352.75	10.38		352.95	14.22
	363.17	8.27		363.15	10.62		363.15	14.29
	Soft-SAFT EoS binary parameters							
	T^a (K)	η	T^a (K)	η		T^a (K)	η	
	293.21	1.0520	323.24	1.0555		353.15	1.0628	
	303.13	1.0523	333.15	1.0575		363.18	1.0657	
	313.28	1.0535	343.14	1.0599				

[a] Average temperature.

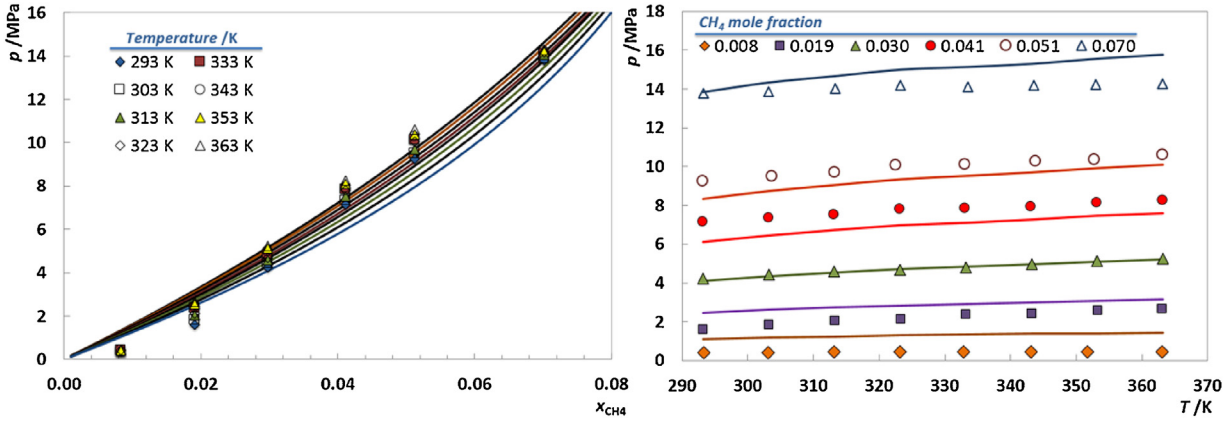

Fig. 3. *pTx* diagrams and modeling results for the system CH_4 + [C_4C_1im][[N(CN)$_2$]. The solid lines represent the soft-SAFT results.

Table 4
Bubble point data of the system N_2 + [C_4C_1im][N(CN)$_2$].

x_{N_2}	T (K)	P (MPa)	x_{N_2}	T (K)	p (MPa)	x_{N_2}	T (K)	p (MPa)
$m = 0.079\ mol_{N_2} \cdot kg_{IL}^{-1}$			$m = 0.235\ mol_{N_2} \cdot kg_{IL}^{-1}$			$m = 0.343\ mol_{N_2} \cdot kg_{IL}^{-1}$		
0.016	293.93	8.341	0.045	293.63	40.519	0.061	293.58	62.746
	303.28	8.183		303.17	37.475		303.55	57.185
	313.26	7.969		313.36	34.875		313.26	53.502
	323.14	7.694		322.96	32.617		322.89	50.773
	332.98	7.404		333.55	31.183		332.58	48.440
	343.19	7.216		343.24	29.567		342.60	45.705
	353.11	7.082		353.37	28.297		353.23	41.936
	363.26	6.863		363.50	27.375		363.16	39.977
$m = 0.481\ mol_{N_2} \cdot kg_{IL}^{-1}$						**Soft-SAFT EoS binary parameters**		
0.083	–	–				$\xi = 0.88$		
	–	–						
	–	–						
	323.57	68.484						
	333.96	63.732						
	343.68	60.374						
	353.28	58.386						
	363.03	55.026						

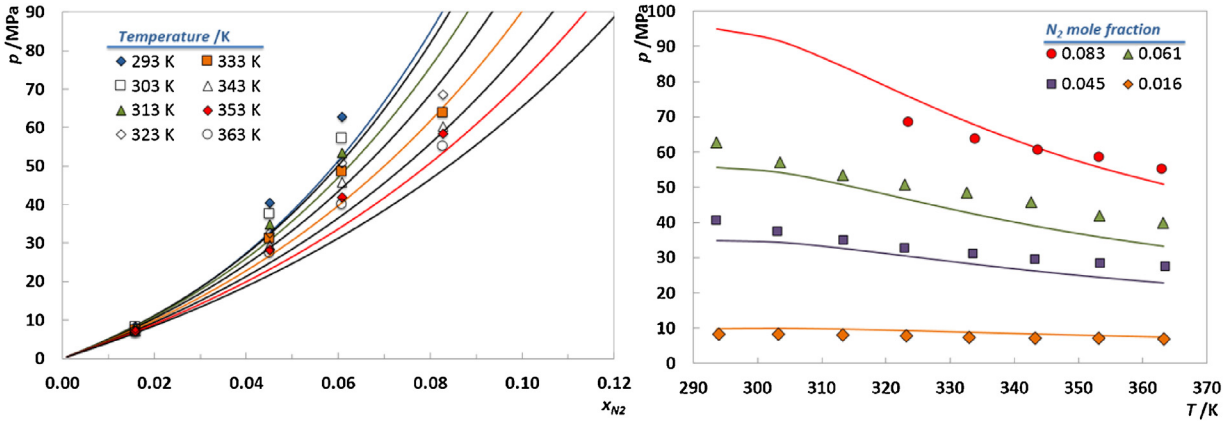

Fig. 4. *pTx* diagrams and modeling results for the system N_2 + [C_4C_1im][[N(CN)$_2$]. The solid lines represent the soft-SAFT EoS results using a temperature independent energy binary interaction parameter.

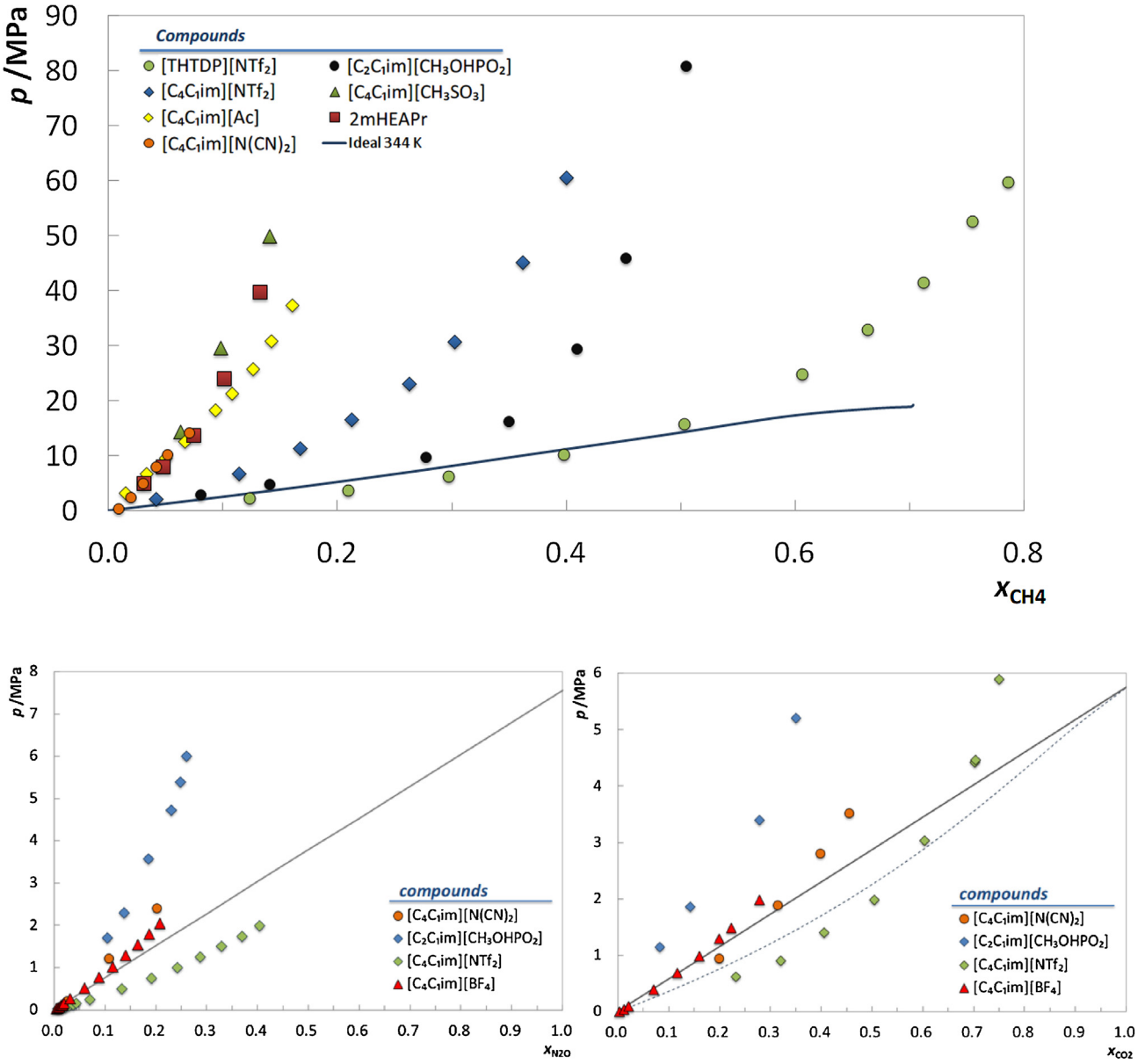

Fig. 5. *pTx* diagram for the system CH_4 + ILs at 343 K (top) [10], N_2O + ILs at 298 K (bottom left) and CO_2 + ILs at 298 K [23,29,32]. The solid line represents the ideal behavior and the dashed line the Flory–Huggins model.

Table 5
Estimated Henry's law constants (MPa)for CO_2, N_2O, CH_4 and N_2 in $[C_4C_1im][N(CN)_2]$.

	T (K)							
	293.15	303.15	313.15	323.15	333.15	343.15	353.15	363.15
CO_2	8.48	9.38	11.08	13.24	14.35	15.97	17.57	19.18
N_2O	8.05	9.66	11.26	12.78	14.29	15.77	17.25	18.72
CH_4	120.28	127.67	133.93	139.69	143.94	148.03	152.48	156.32
N_2	460.18	470.78	466.83	454.53	437.76	420.01	402.09	385.16

Table 6
Selectivities for CO_2, N_2O, CH_4 and N_2 in ILs and some common solvents at 298 K.

	H_{CO_2}/MPa	H_{N_2O} /MPa	H_{N_2}/MPa	H_{CH_4}/MPa	$S_{CO_2/N2}$	S_{N_2O/N_2}	S_{CO_2/N_2O}	S_{CH_4/N_2}	S_{CO_2/CH_4}	Ref.
$[C_4C_1im][N(CN)_2]$	8.98	8.87	466.77	124.13	51.97	52.65	0.99	3.76	13.82	This work[a]
$[C_2C_1im][CH_3OHPO_2]$	7.74	14.18	958.47	192.78	123.86	67.58	1.83	4.97	24.91	[23]
$[C_2C_1im][BF_4]$	8.0		710.0	290.0	88.8			2.4	36.3	[38]
$[C_4C_1im][BF_4]$	5.38	7.86					1.46			[29]
$[C_2C_1im][N(CN)_2]$	96.0[b]		490.0[b]	200.0[b]	51.03[b]	57.13[b]		2.45[b]	20.83[b]	[39]
$[C_2C_1im][NTf_2]$	3.9		140.0	58.0	35.9			2.4	14.9	[38]
$[C_4C_1im][NTf_2]$	1.62	3.21					1.98			[29]
$[C_6C_1im][NTf_2]$	3.4		100.0	35.0	29.4			2.9	10.3	[38]
$[C_4C_1im][SCN]$	10.28	12.78					1.24			[29]
MEA (40 wt%)					25.67[c]			3.33[c]	7.70[c]	[33]
CH_3OH					23.00			3.19	7.20	[34]
TEGMME	7.50	8.10		85.03					11.34	[35–37]

[a] Interpulated values.
[b] Values taken from Camper et al. [39] at 313 K.
[c] Values taken from Xu et al. [33] at 303 K.

4.4. Deviations to ideality

Following the approach used in previous works [10–12,23], the mechanism behind the solubility of the gases of interest in ionic liquids was investigated by analyzing their deviations from ideality in the liquid phase. The system CH_4 + hexane [31], an athermic, quasi-ideal mixture, with negligible enthalpic interactions and reduced entropic contributions resulting from the differences in size and shape of the species, was adopted to describe the methane ideal behavior.

As depicted in Fig. 5, $[C_4C_1im][[N(CN)_2]$ presents positive deviations from ideality for both CH_4 and N_2O that result from positive deviations in the residual (enthalpic) term. Furthermore, for methane, the studied IL presents strong positive deviations from ideality similar to those reported previously [10] for $[C_4C_1im][Ac]$, N-methyl-2-hydroxyethylammonium propionate (2mHEAPr) or $[C_4C_1im][CH_3SO_3]$ ILs.

4.5. Selectivities

The ideal gas selectivities ($S_{1/2}$) were evaluated for the four gases studied in this work using the Henry's constants calculated from the soft-SAFT EoS, following the approach used in previous works [10,23] and according to the following equation:

$$S_{1/2} = \frac{H_{2,IL}}{H_{1,IL}} \tag{2}$$

where $H_{i,IL}$ stands for the Henry's constant of gas 1 and 2 in the *IL*.

The Henry's law relates the amount of a given gas dissolved in a liquid, at a constant temperature, to the fugacity of that gas in equilibrium with that liquid and can be described as:

$$H_{i,IL}(T,p) = \lim_{x_i \to 0} \frac{f_i^{IL}}{x_i} \tag{3}$$

where $H_{i,IL}$ (T, p) is the Henry's constant, x_i is the mole fraction of gas i dissolved in the ionic liquid, and f_i^{IL} is the fugacity of the gas i in the ionic liquid phase (*IL*). Eq. (3) is only rigorously valid in the diluted region limit. The Henry's constants were estimated by fitting the soft-SAFT EoS to the experimental data and calculating the limiting slope as the solubility approaches zero. Although this procedure introduces some uncertainty on the estimated Henry's constants, the results obtained for the gases are different enough to allow a discussion on the solvation of the gases on the IL and are reported in Table 5.

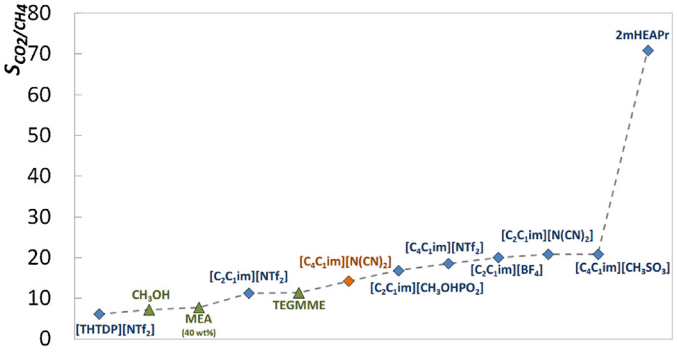

Fig. 6. CO_2/CH_4 selectivities of ILs, methanol, MEA (40 wt%) and TEGMME at 313 K.

The calculated Henry's constant for the studied gases in $[C_4C_1im][N(CN)_2]$, at a selected temperature of 298 K, were further compared with the Henry's constants of the same gases in other ILs, such as 1-ethyl-3-methylimidazolium tetrafluoroborate ($[C_2C_1im][BF_4]$), 1-butyl-3-methylimidazolium tetrafluoroborate ($[C_4C_1im][BF_4]$), 1-ethyl-3-methylimidazolium dicyanamide ($[C_2C_1im][N(CN)_2]$), 1-butyl-3-methylimidazolium dicyanamide ($[C_4C_1im][N(CN)_2]$), 1-ethyl-3-methylimidazolium bis(trifluoromethylsulfonyl)imide ($[C_2C_1im][NTf_2]$), 1-butyl-3-methylimidazolium bis(trifluoromethylsulfonyl)imide ($[C_4C_1im][NTf_2]$), 1-hexyl-3-methylimidazolium bis(trifluoromethylsulfonyl)imide ($[C_6C_1im][NTf_2]$), 1-ethyl-3-methylimidazolium methylphosphonate ($[C_2C_1im][CH_3OHPO_2]$) and 1-butyl-3-methylimidazolium thiocyanate ($[C_4C_1im][SCN]$), as well as in other solvents commonly used for CO_2 capture, such as glycol monoethyl ether (TEGMME), methanol (CH_3OH) and aqueous solutions of MEA (40 wt%).

The results, reported in Tables 5 and 6, show that the solubility of N_2 is very low in most ILs (high Henry's law constants) and therefore high selectivity towards carbon dioxide and nitrous oxide can be achieved when compared to traditional solvents. Nonetheless, although the solubility of CH_4 in $[C_4C_1im][N(CN)_2]$ is similar to that of other size-equivalent ILs, its CO_2 solubility is lower, leading to one of the lowest selectivities reported for ILs, as depicted in Fig. 6. A similar behavior has been previously reported for $[C_2C_1im][CH_3OHPO_2]$ [23] and is an indication of the unfavorable interactions of IL—CH_4, CO_2, N_2O and N_2 present on highly polar ILs systems. These results indicate that, a delicate balance between the solvent polarity and its molar volume must be ascertained when targeting a highly selective solvent for CO_2/N_2, CO_2/CH_4 or N_2O/CH_4 separation.

5. Conclusions

The knowledge and understanding of the solubility of gases in ILs in a wide range of molar fractions, temperatures and pressures is essential for the adequate development and optimization of ILs-based processes for greenhouse gases capture or natural gas streams purification. Aiming to achieve enhanced carbon dioxide and nitrous oxide selectivity towards methane and nitrogen, N_2O, N_2 and CH_4 gas–liquid equilibrium data in the highly polar 1-butyl-3-methylimidazolium dicyanamide ionic liquid was evaluated in the 293–363 K temperature range and for pressures up to 70 MPa. Although N_2 and CH_4 solubilities in $[C_4C_1im][N(CN)_2]$ are very low, presenting positive deviations to ideality similar to that of other size-equivalent ILs, its CO_2 and N_2O solubilities are lower than expected leading to selectivities slightly higher than those of traditional solvents. This behavior has been reported in a previous publication for other highly polar IL and it is an indication of the unfavorable interactions of this IL towards the studied gases. This behavior evidences that a delicate balance between the solvent polarity and its molar volume must be ascertained when searching for a highly selective solvent for N_2 or CH_4 separation.

The soft-SAFT EoS was used to describe the high pressure phase behavior of the studied systems. The molecular model and parameters sets reported in a previous publication for $[C_4C_1im][N(CN)_2]$ were used in a transferable manner, allowing a good description of the binary systems studied, including the small CH_4 temperature dependency and the N_2 reverse temperature dependency on the solubility. To accurately describe the $N_2 + [C_4C_1im][N(CN)_2]$ system, the size binary parameter had little influence in the model results while a temperature independent energy binary interaction parameter was required to correctly describe the GLE data. On the contrary, for the $CH_4 + [C_4C_1im][N(CN)_2]$ binary system, the energy binary interaction parameter had little influence in the model results, meaning that the model is able to correctly take into account the weak interactions between methane and $[C_4C_1im][[N(CN)_2]$. However, this system requires the inclusion of a temperature dependent size binary interaction parameter in order to better describe the small temperature dependency observed for the solubility of methane in $[C_4C_1im][[N(CN)_2]$. These results again confirm that the soft-SAFT EoS stands as a prominent and powerful tool for the development and optimization of high pressure CCS processes using ionic liquids, when experimental data is not available.

Acknowledgments

This work was developed in the scope of the project CICECO-Aveiro Institute of Materials, POCI-01-0145-FEDER-007679 (FCT ref. UID/CTM/50011/2013), financed by national funds through the FCT/MEC and co-financed by FEDER under the PT2020 Partnership Agreement. This work has been partially financed by the Catalan government (project 2014-SGR1582) and the Spanish Government (project CTQ2014-53987-R). P.J.C. and M.B.O. acknowledge FCT for their post-doctoral grants SFRH/BPD/82264/2011 and SFRH/BPD/71200/2010, respectively. A.M.A. Dias acknowledges FCT-MEC for contract Investigador FCT IF/00455/2013

References

[1] L. Raynal, P.-A. Bouillon, A. Gomez, P. Broutin, From MEA to demixing solvents and future steps, a roadmap for lowering the cost of post-combustion carbon capture, Chem. Eng. J.V 171 (2011) 742–752.
[2] D. Zhu, M. Fang, Z. Lv, Z. Wang, Z. Luo, Selection of blended solvents for CO_2 absorption from coal-fired flue gas. Part 1: Monoethanolamine (MEA)-based solvents, Energy Fuels 26 (2012) 147–153.
[3] M. Poloncarzova, J. Vejrazka, V. Vesely, P. Izak, Effective purification of biogas by a condensing-liquid membrane, Angew. Chem. Int. Ed. 50 (2011) 669–671, in English.
[4] P. Scovazzo, D. Havard, M. McShea, S. Mixon, D. Morgan, Long-term, continuous mixed-gas dry fed CO_2/CH_4 and CO_2/N_2 separation performance and selectivities for room temperature ionic liquid membranes, J. Membr. Sci. 327 (2009) 41–48.
[5] X. Zhang, W.S. Seames, B.M. Tande, Recovery of CO_2 from monoethanolamine using a membrane contactor, Sep. Sci. Technol.V 49 (2014) 1–11.
[6] D. Morgan, L. Ferguson, P. Scovazzo, Diffusivities of gases in room-temperature ionic liquids: data and correlations obtained using a lag-time technique, Ind. Eng. Chem. Res. 44 (2005) 4815–4823.
[7] R. Condemarin, P. Scovazzo, Gas permeabilities, solubilities, diffusivities, and diffusivity correlations for ammonium-based room temperature ionic liquids with comparison to imidazolium and phosphonium RTIL data, Chem. Eng. J. 147 (2009) 51–57.
[8] J.E. Bara, T.K. Carlisle, C.J. Gabriel, D. Camper, A. Finotello, D.L. Gin, R.D. Noble, Guide to CO_2 separations in imidazolium-based room-temperature ionic liquids, Ind. Eng. Chem. Res. 48 (2009) 2739–2751.
[9] L. Ferguson, P. Scovazzo, Solubility, diffusivity, and permeability of gases in phosphonium-based room temperature ionic liquids: data and correlations, Ind. Eng. Chem. Res. 46 (2007) 1369–1374.
[10] P.J. Carvalho, J.A.P. Coutinho, The polarity effect upon the methane solubility in ionic liquids: a contribution for the design of ionic liquids for enhanced CO_2/CH_4 and H_2S/CH_4 selectivities, Energy Environ. Sci. 4 (2011) 4614–4619.
[11] P.J. Carvalho, J.A.P. Coutinho, Non-ideality of solutions of NH_3, SO_2, and H_2S in ionic liquids and the prediction of their solubilities using the Flory–Huggins model, Energy Fuels 24 (2010) 6662–6666.
[12] P.J. Carvalho, J.A.P. Coutinho, On the nonideality of CO_2 solutions in ionic liquids and other low volatile solvents, J. Phys. Chem. Lett. 1 (2010) 774–780.
[13] F.J. Blas, L.F. Vega, Prediction of binary and ternary diagrams using the Statistical Associating Fluid Theory (SAFT) equation of state, Ind. Eng. Chem. Res. 37 (1998) 660–674.
[14] F.J. Blas, L.F. Vega, Thermodynamic behaviour of homonuclear and heteronuclear Lennard-Jones chains with association sites from simulation and theory, Mol. Phys.V 92 (1997) 135–150.
[15] L.F. Vega, O. Vilaseca, F. Llovell, J.S. Andreu, Modeling ionic liquids and the solubility of gases in them: recent advances and perspectives, Fluid Phase Equilib. 294 (2010) 15–30.
[16] L.M.C. Pereira, M.B. Oliveira, F. Llovell, L.F. Vega, J.A.P. Coutinho, Assessing the N_2O/CO_2 high pressure separation using ionic liquids with the soft-SAFT EoS, J. Supercrit. Fluids 92 (2014) 231–241.
[17] C.M.S.S. Neves, K.A. Kurnia, J.A.P. Coutinho, I.M. Marrucho, J.N.C. Lopes, M.G. Freire, L.P.N. Rebelo, Systematic study of the thermophysical properties of imidazolium-based ionic liquids with cyano-functionalized anions, J. Phys. Chem. B 117 (2013) 10271–10283.
[18] H.F.D. Almeida, P.J. Carvalho, K.A. Kurnia, J.A. Lopes-da-Silva, J.A.P. Coutinho, M.G. Freire, Surface tensions of ionic liquids: a non-regular trend along the number of cyano groups fluid phase equilibria, Fluid Phase Equilib. 409 (2015) 458–465.
[19] M.L.S. Batista, K.A. Kurnia, S.P. Pinho, J.R.B. Gomes, J.A.P. Coutinho, Computational and experimental study of the behavior of cyano-based ionic liquids in aqueous solution, J. Phys. Chem. B 119 (2015) 1567–1578.
[20] A.M.A. Dias, H. Carrier, J.L. Daridon, J.C. Pàmies, L.F. Vega, J.A.P. Coutinho, I.M. Marrucho, Vapor–liquid equilibrium of carbon dioxide–perfluoroalkane mixtures: experimental data and SAFT modeling, Ind. Eng. Chem. Res. 45 (2006) 2341–2350.
[21] N. Pedrosa, J.C. Pàmies, J.A.P. Coutinho, I.M. Marrucho, L.F. Vega, Phase equilibria of ethylene glycol oligomers and their mixtures, Ind. Eng. Chem. Res. 44 (2005) 7027–7037.
[22] J.C. Pàmies, L.F. Vega, Vapor–liquid equilibria and critical behavior of heavy *n*-alkanes using transferable parameters from the soft-SAFT equation of state, Ind. Eng. Chem. Res. 40 (2001) 2532–2543.
[23] L.M.C. Pereira, M.B. Oliveira, A.M.A. Dias, F. Llovell, L.F. Vega, P.J. Carvalho, J.A.P. Coutinho, High pressure separation of greenhouse gases from air with 1-ethyl-3-methylimidazolium methyl-phosphonate, Int. J. Greenhouse Gas Control V 19 (2013) 299–309.

[24] J.S. Andreu, L.F. Vega, Capturing the solubility behavior of CO_2 in ionic liquids by a simple model, J. Phys. Chem. C 111 (2007) 16028–16034.
[25] P.J. Carvalho, V.H. Álvarez, J.J.B. Machado, J. Pauly, J.-L. Daridon, I.M. Marrucho, M. Aznar, J.A.P. Coutinho, High pressure phase behavior of carbon dioxide in 1-alkyl-3-methylimidazolium bis(trifluoromethylsulfonyl)imide ionic liquids, J. Supercrit. Fluids 48 (2009) 99–107.
[26] S. Vitu, J.N. Jaubert, J. Pauly, J.L. Daridon, D. Barth, Phase equilibria measurements of CO_2 + methyl cyclopentane and CO_2 + isopropyl cyclohexane binary mixtures at elevated pressures, J. Supercrit. Fluids 44 (2008) 155–163.
[27] J. Pauly, J. Coutinho, J.L. Daridon, High pressure phase equilibria in methane + waxy systems: 1. methane + heptadecane, Fluid Phase Equilib. 255 (2007) 193–199.
[28] P.J. Carvalho, V.H. Álvarez, I.M. Marrucho, M. Aznar, J.A.P. Coutinho, High pressure phase behavior of carbon dioxide in 1-butyl-3-methylimidazolium bis(trifluoromethylsulfonyl)imide and 1-butyl-3-methylimidazolium dicyanamide ionic liquids, J. Supercrit. Fluids 50 (2009) 105–111.
[29] M.B. Shiflett, A.M.S. Niehaus, B.a. Elliott, A. Yokozeki, Phase behavior of N_2O and CO_2 in room-temperature ionic liquids [bmim][Tf2N], [bmim][BF4], [bmim][$N(CN)_2$], [bmim][Ac], [eam][NO_3], and [bmim][SCN], Int. J. Thermophys. 33 (2012) 412–436.
[30] J. Kumełan, Á. Pérez-Salado Kamps, D. Tuma, G. Maurer, Solubility of the single gases H_2 and CO in the ionic liquid [bmim][CH_3SO_4], Fluid Phase Equilib. 260 (2007) 3–8.
[31] R.S. Poston, J.J. McKetta, Vapor–liquid equilibrium in the methane-*n*-hexane system, J. Chem. Eng. Data V 11 (1966) 362–363.
[32] M.B. Shiflett, A.M.S. Niehaus, A. Yokozeki, Separation of N_2O and CO_2 using room-temperature ionic liquid [bmim][BF4], J. Phys. Chem. B 115 (2011) 3478–3487.
[33] X. Xu, X. Zhao, L. Sun, X. Liu, Adsorption separation of carbon dioxide, methane and nitrogen on monoethanol amine modified β-zeolite, J. Nat. Gas Chem. 18 (2009) 167–172.
[34] H. Lin, B.D. Freeman, Materials selection guidelines for membranes that remove CO_2 from gas mixtures, J. Mol. Struct. 739 (2005) 57–74.
[35] A. Henni, A.E. Mather, The solubility of CO_2 in triethylene glycol monomethyl ether, Can. J. Chem. Eng. 73 (1995) 156–158.
[36] A. Henni, A.E. Mather, Solubility of nitrous oxide in triethylene glycol monomethyl ether at elevated pressures, J. Chem. Eng. Data 40 (1995) 1158–1160.
[37] A. Henni, A.E. Mather, The solubility of methane in triethylene glycol monomethyl ether, Fluid Phase Equilib. 108 (1995) 213–218.
[38] A. Finotello, J.E. Bara, D. Camper, R.D. Noble, Room-temperature ionic liquids: temperature dependence of gas solubility selectivity, Ind. Eng. Chem. Res. 47 (2007) 3453–3459.
[39] D. Camper, J. Bara, C. Koval, R. Noble, Bulk-fluid solubility and membrane feasibility of rmim-based room-temperature ionic liquids, Ind. Eng. Chem. Res. 45 (2006) 6279–6283.